Evaluation of respiratory- and postural-induced changes on the ballistocardiogram signal by time warping averaging.

A Martín-Yebra[1,2], F. Landreani[1], C. Casellato[1], E. Pavan[1], P-F Migeotte[3], C. Frigo[1], J P Martínez[2,4], E G Caiani[1]

1. Dipartimento di Elettronica, Informazione e Bioingegneria, Politecnico di Milano, Milano, Italy; {albapilar.martin, enrico.caiani}@polimi.it
2. BSICoS Group, Instituto de Investigación en Ingeniería de Aragón (I3A), IIS Aragón, Universidad de Zaragoza, Zaragoza, Spain;
3. Laboratory of Physics and Physiology, Université Libre de Bruxelles, Bruxelles, Belgium;
4. Centro de Investigación Biomédica en Red - Bioingeniería, Biomateriales y Nanomedicina, Zaragoza, Spain.

Corresponding author:

Enrico G. Caiani, PhD

Politecnico di Milano, Dipartimento di Elettronica, Informazione e Bioingegneria

Piazza Leonardo da Vinci 32,

20.133, Milano, Italy

Fax +39 02.2399.3360; tel. +39 02 2399.3390

e-mail: enrico.caiani@polimi.it

Abstract

Objective: The aim of this work was to evaluate the potential changes in the ballistocardiogram (BCG) signal induced by different respiratory patterns and posture, by using the dynamic time warping (DTW) technique.

Approach: BCG signals were recorded in a group of 20 healthy volunteers, simultaneously to the ECG. Two recordings, one in supine (SUP) and one in standing (ST) position, including spontaneous breathing, two 1-minute apneas (at full and empty-lungs, respectively) and 30s of Valsalva, were analyzed. A warped averaged waveform was computed for each phase, from which amplitude and temporal parameters were extracted to characterize each condition.

Main results: variations in both amplitude and duration BCG-derived parameters among manoeuvres, especially when compared to spontaneous breathing were found, suggesting a complex interaction between intrathoracic pressure changes, acting on venous return together with the autonomic nervous system modulation on heart rate. Also the effect of hydrostatic pressure gradient elicited by postural conditions was evident.

Significance: Posture and respiratory manoeuvres affect the BCG signal in different ways, probably as a result of changes induced in preload and afterload. This supports the need in defining separate normality ranges for each posture and/or breathing conditions, as well as the importance of applying specific manoeuvres to highlight any pathological response in the computed BCG parameters.

Keywords: Ballistocardiogram (BCG); signal averaging; dynamic time warping (DTW); cardiac monitoring; respiration.

1. Introduction

Ballistocardiography (BCG) is a non-invasive technique that measures the heart-beat induced mass movements of circulating blood and of the heart itself, generated by the acceleration of blood as it is ejected and moved to the aorta and the large vessels (Gubner et al., 1953). It is represented by a succession of systolic (H, I, J, K) and diastolic (L, M, N) waves, describing the forces associated to the shifting of the centre of mass of the body throughout the cardiac cycle (Pinheiro et al., 2010). BCG has been recently reconsidered as a useful technique to characterize cardiac performance (Inan et al., 2015), offering a simple, efficient and affordable solution for home e-health monitoring (Javaid et al., 2016), potentially representing an important practice for preventing and early-detecting cardiac-related diseases.

Temporal parameters, as the RJ interval (the time interval between the occurrence of the R-peak on the ECG signal and the corresponding J wave on the BCG), has been proposed as a surrogate of the pre-ejection period (PEP) to non-invasively assess cardiac contractility (Etemadi et al., 2011; Inan et al., 2008; Javaid et al., 2016). On the other hand, the amplitude of the BCG signal, especially in systolic waves, was mainly correlated with cardiac output, cardiac force and velocity of ejection (Starr et al., 1939), and has been found to be an indicator of myocardial contraction force (Starr, 1965, 1955).

However, the BCG quasi-periodic signal is characterized by a large inter-beat variability in its morphology (both in duration and amplitude), mainly related to the respiratory activity and mediated by the autonomic nervous system, thus affecting both preload and afterload by changes in intrathoracic pressure.

In order to extract valuable information from the BCG signal, two different approaches have been proposed: 1) to extract beat-by-beat series from short-term (>= 3 minutes) recordings in order to characterize time and frequency parameters of heart-rate variability (Shin et al., 2011; Zhu et al., 2012); 2) to average consecutive beats acquired over shorter sequences (< 1 min) in order to obtain a characteristic waveform from which deriving indices of cardiac performance (Etemadi et al., 2011; He et al., 2011).

With regard to the averaging of biological signals, three different approaches are available: synchronous, template-based, and non-linear techniques. Synchronous averaging is extensively used when a stimulus is present and the system's response is supposed to be stationary, where the waveforms are averaged after being aligned with respect to a reference point (Cohen, 1986). The template-based approach is based on *a priori* selection of a reference waveform (i.e., the template) which is used to filter out non similar waveforms from the signal, thus resulting in the averaging of the remaining similar ones (Aunon et al., 1980). Finally, non-linear averaging techniques have been proposed to solve the limitations related to the previous methods, in particular when dealing with quasi-periodic biological signals, whose morphology varies both in amplitude and duration.

In particular, the dynamic time warping (DTW) technique, originally proposed with success for speech recognition (Sakoe and Chiba, 1978), has been already applied to an echo-derived left ventricular volume signal for the assessment of its function (Caiani et al., 2002). A potential of this technique is that it allows performing the averaging operation after finding the best alignment between consecutive waveforms, thus compensating temporal distortions without any *a priori* information.

We hypothesised that the use of the DTW algorithm could be successfully applied to the BCG signal to obtain an average waveform from a sequence of consecutive beats from which to extract amplitude and temporal parameters to characterize cardiac performance.

In order to define a proper acquisition protocol that could then be implemented in a home-monitoring scenario, our aim was to evaluate the potential changes in the BCG signal induced by different postural conditions, as well as during different respiratory manoeuvres.

2. Materials and methods

2.1. Study protocol and population

Three-orthogonal components of the BCG signal, denoted as AP (Anterior-Posterior), LR (Left-Right, mediolateral), and HF (Head-Foot, longitudinal), were acquired (sampling frequency 960 Hz) by using a multicomponent biomechanical force plate, based on 3D piezoelectric load cells (Type 9286B, Kistler®, 600 x 400 mm), placed on the floor with the top surface 40mm above the floor level. Moreover, the experimental set-up included a rigid wooden platform (length 2100, width 400, height 40 mm) placed over the force plate, with its centre in correspondence to the centre of the force plate and parallel to the horizontal plane, in order to avoid any contact with the floor. Forces induced by the body mass micro-displacements were directly transferred to the force plate, being this able to capture magnitude changes as small as 0.01N. An offset-reset of the force platform was performed at the onset of each acquisition allowing both the body weight and the wooden platform weight (i.e., the continuous signal component) to be automatically removed.

Simultaneously, a standard three-lead ECG signal was collected by a portable system (Porti TMSiTM, sampling frequency of 2048 Hz). The ECG and BCG signals were synchronized by using a TTL function generator that sent a signal simultaneously acquired by both systems.

Subjects were first asked to stay in supine (SUP) position, with their centre of mass aligned with the central point of the force plate (Figure 1.a), and then in standing (ST) position, with their feet centrally positioned (Figure 1.b). Our acquisition protocol included two consecutive recordings (SUP and ST, respectively), each consisting of:

a) 5 minutes at resting conditions.

b) 3 preparatory deep breaths.

c) 1-minute apnea at end-inspiration (Full-lung apnea).

d) 1 minute of normal breathing.

e) 3 preparatory deep breaths.

f) 1-minute apnea at end-expiration (Empty-lung apnea).

g) 1 minute of normal breathing.

h) 30 seconds of Valsalva manoeuvre.

Subjects were asked to stay quiet, without voluntary movements, along the whole acquisition in order to minimize motion artefacts and to ensure that the signal oscillations were mainly due to mass motion inside the body.

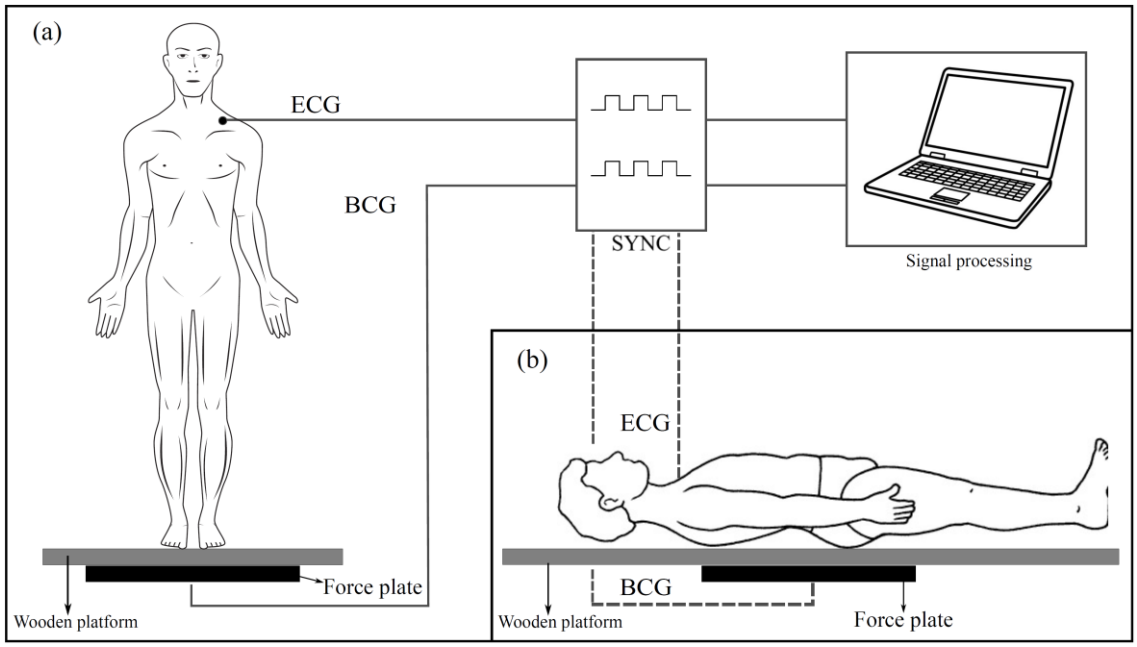

Figure 1: Schematic of the experimental set up for the subject in standing position (a) and in supine (b).

The analysed population was a group of 20 healthy volunteers (12 females) whose main characteristics are summarised in table 1.

Table 1: Study population characteristics expressed as mean ± std.

Variable	**Males**	**Females**
Age (years)	32.9 ± 9.0	28.2 ± 4.8
Weight (kg)	72.9 ± 10.5	53.9 ± 8.3
Height (m)	1.79 ± 0.08	1.62 ± 0.06
BMI (kg/m^2)	22.8 ± 4.06	20.6 ± 2.13

BMI: body mass index.

All participants gave written informed consent to participate in the study. The experimental procedures involving healthy volunteers described in this paper were in agreement with the principles outlined in the Helsinki Declaration of 1975, as revised in 2013. Ethical committee approval of Université Libre de Bruxelles, Hopital Erasme, was obtained prior to the study.

2.2. Pre-processing

The pre-processing stage included automatic QRS detection from the ECG signal using a wavelet-based ECG delineator (Martinez et al., 2004), followed by ECG-BCG synchronization using the trigger signal. The BCG signal was then filtered (band pass, 0.1-30 Hz, Butterworth filter, order 8) in order to remove baseline wander, noise and other out-of-band components (high-frequency motion artifacts).

Figure 2 shows an example of the three orthogonal filtered components of the reaction force from a representative subject, in supine (upper panel) and standing (bottom panel) positions, synchronized with the ECG signal. It is possible to notice that in both postures the best signal-to-noise ratio, and the most informative content showing the quasi-periodic heart-induced activity, was visible in the longitudinal head-to-foot (HF) component. Based on this consideration together with the fact that it has been the most widely-studied component and the only one for which an interpretation has been provided, we focused our attention on this component only.

Finally, BCG segments of the acquisition relevant to phases a), c), f) and h) of the protocol were extracted. R-peak events on the ECG were utilized to delimit each BCG cardiac cycle.

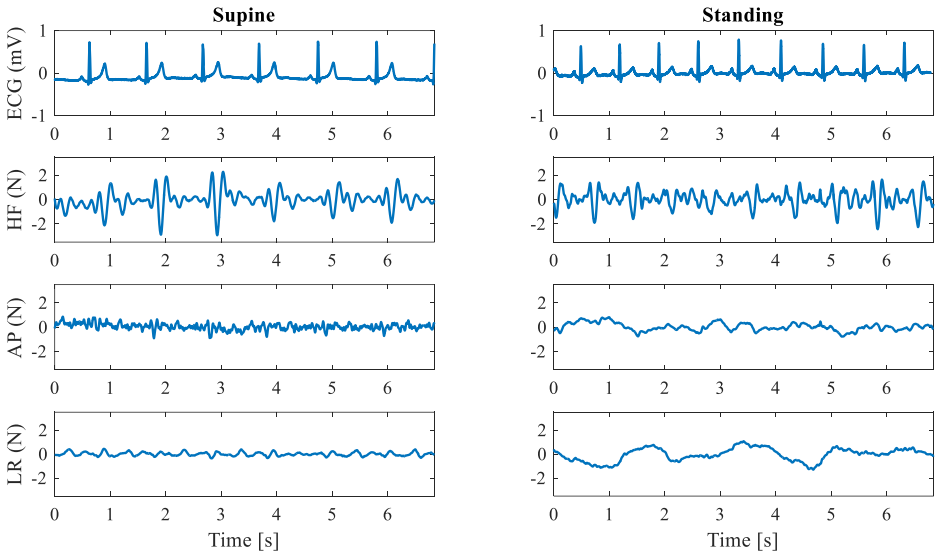

Figure 2: Example of synchronized ECG (mV) and the three components of the BCG signal: HF (head-to-foot), AP (antero-posterior) and LR (left-to-right) components (N), in both supine (left) and standing (right) positions.

2.3. Dynamic time warping

The DTW averaging technique (Sakoe and Chiba, 1978) consists in iterating two consecutive steps performed on pairs of BCG waveforms, each representing one cardiac cycle, according to a binary tree combination procedure:

1. the calculation of the time-warping function (TWF) to perform the best alignment between their temporal axes;
2. the computation of a new waveform by mixing and averaging the values from the two original cycles, according to the TWF.

Calculation of the TWF

A more detailed description of the computation of the TWF can be found elsewhere (Caiani et al., 2002). Summarizing, given two BCG waveforms, $S_x(n)$ and $S_y(m)$, with different duration ($1 \leq n \leq N$ and $1 \leq m \leq M$, respectively) but equally sampled, the temporal correspondence

between samples of S_x and S_y is defined by the monotonic and continuous TWF, matching the time axis *n* of the waveform S_x in the time axis *m* of the waveform S_y, and vice-versa. Figure 2 shows an example of the TWF represented in the plane (n, m), with the patterns S_x and S_y on the *n* and *m* axes, respectively.

To calculate the TWF, the following measure of dissimilarity (i.e. the local cost) between the normalised waveforms S_x and S_y was utilised, as described in (Caiani et al., 2002), taking into account their amplitude and first derivative differences:

$$d(n,m) = k_1\left|S_x(n) - S_y(m)\right| + k_2\left|\dot{S}_x(n) - \dot{S}_y(m)\right|$$

with $k_1 = k_2 = 1$, and $\dot{S}$ representing the first normalized derivative. The value of $d(n,m)$ is computed at every point of the warping plane (n,m) that lies inside the zone of the plane (n,m) around the main diagonal, defined as $|n-m| \leq r$, where $r = 10 + |N-M|$, thus preventing excessive adjustment of the time axes.

Then, given the local dissimilarity $d(n,m)$, by a dynamic programming algorithm (Sakoe and Chiba, 1978) a cost matrix D was computed using the symmetric form without slope constraints (Sakoe and Chiba, 1978), where $D(n,m)$ represents the minimum cumulative cost to reach the point (n,m) starting from (1,1):

$$D(n,m) = min\{D(n,m-1) + d(n,m), D(n-1,m) + d(n,m), D(n-1,m-1) + 2d(n,m)\}$$

with the initial condition of $D(1,1) = 2d(1,1)$ and boundary conditions of $D(n,1) = D(n-1,1) + d(n,1)$ and $D(1,m) = D(1,m-1) + d(1,m)$. The TWF is finally derived as the path with minimum cost from (1,1) to (N,M).

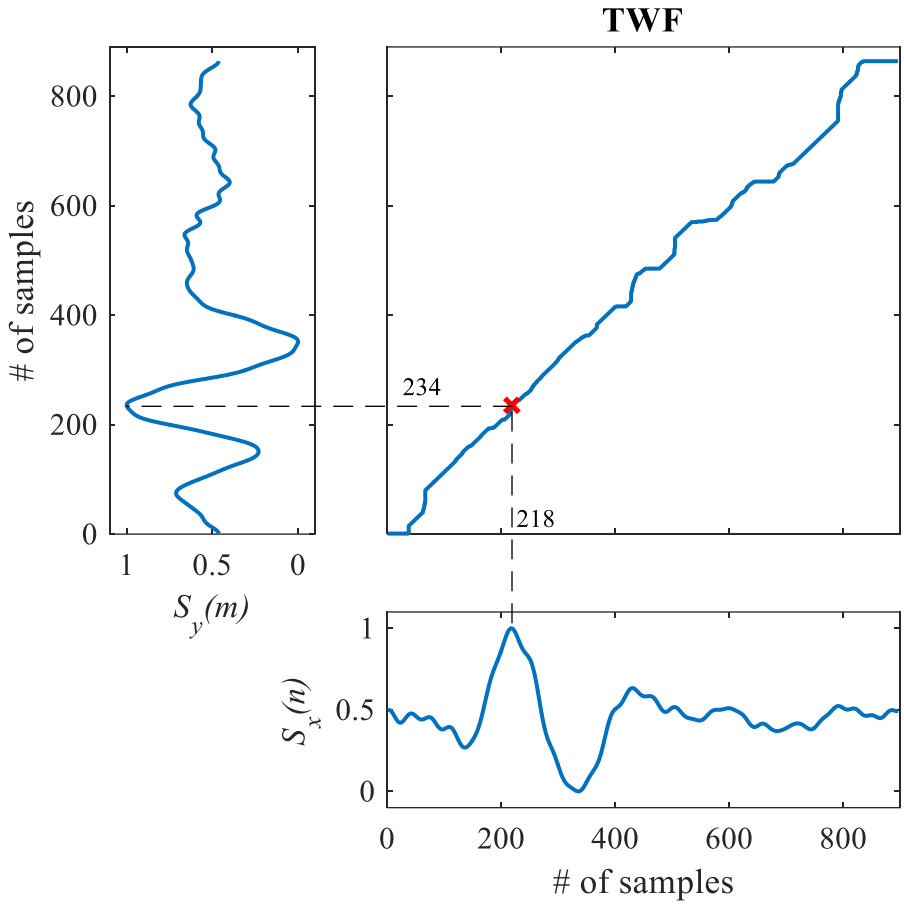

Figure 3: Example of the computed time-warping function (TWF) that best aligns the two consecutive BCG normalized waveforms, here denoted as $S_x(n)$ and $S_y(m)$. The red cross represents the correspondence between the two J positive waves in both waveforms (samples n = 218 and m = 234, respectively).

Computation of the averaged waveform

The warped average (WA) between two consecutive BCG cycles was computed according to the TWF as described in (Caiani et al., 2002), resulting in a waveform of duration equal to $(N + M)/2$. The final WA is computed from a set of L consecutive cycles, being L an integer power of two. Waveforms are grouped in L/2 pairs, resulting in L/2 WAs computed. Then, this step is iterated until just one final WA beat is obtained.

To compare the effects of the different manoeuvres, L=32 consecutive beats were considered for each phase of the protocol (number limited by the shortest phase that is the 30-second Valsalva manoeuvre stage). Figure 3 shows an example of the original 32 consecutive beats obtained in a subject in standing position during the resting period, together with the corresponding synchronous averaging (blue dashed line) and the final warped average (in red). It is possible to notice how the characteristic peaks of the BCG signal were maintained, especially during the diastolic phase, by the proposed DTW averaging technique, despite differences in both amplitude and duration among the considered waveforms. As expected, amplitude and temporal position of the H, I, J, K peaks appeared dependent of the utilized averaging approach.

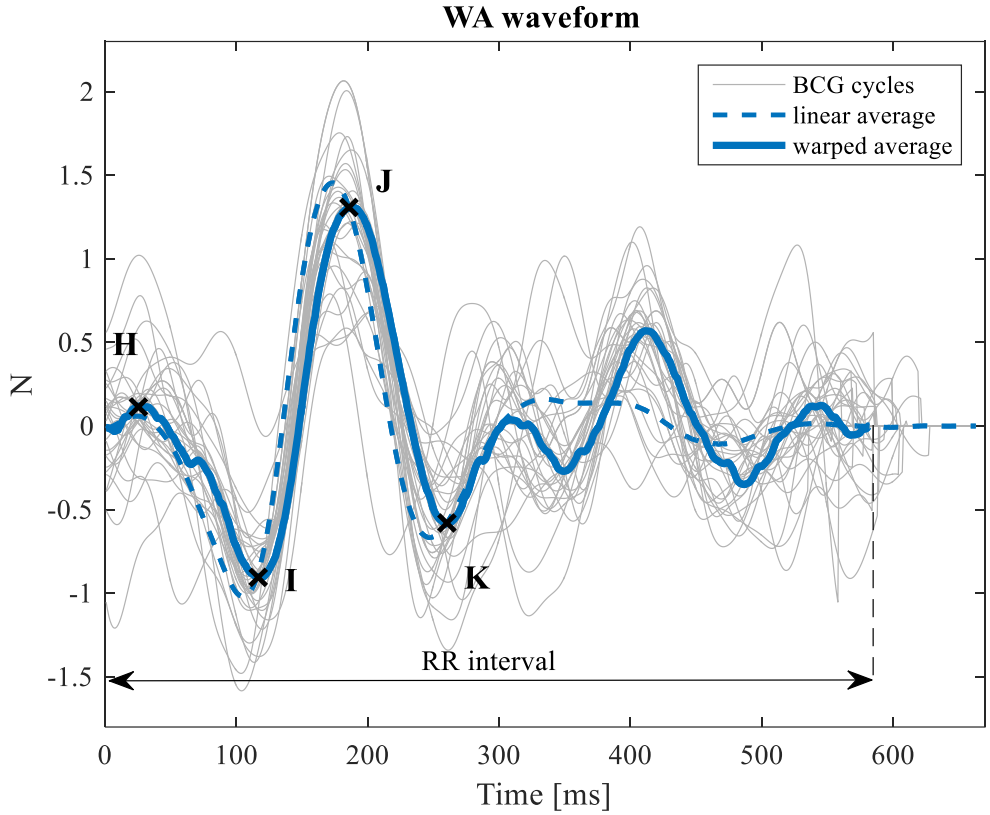

Figure 4: Example of a sequence of 32 BCG waveforms (light blue) obtained in one subject, the result of their synchronous averaging (dark blue dashed line) and of the DTW averaging (in red).

2.4. Fiducial points detection

For each phase of the protocol, that is, resting, full-lung apnea (Full), empty-lung apnea (Emp) and Valsalva (Val), the respective WA waveform was computed.

As the WA represents the temporal average of the 32 consecutive beats, the duration of the template defines the average RR interval. Systolic fiducial points were then identified on each final WA waveform, as shown on Figure 3: according to (Pinheiro et al., 2010) the H wave, represents the first positive peak, synchronous with the isovolumetric contraction; the I wave, that is the first negative wave at the onset of ejection (early systole), corresponds to blood acceleration in the ascending aorta and pulmonary arteries; the J wave, the main positive wave occurring late in systole, corresponds to blood acceleration when ejected into the descending aorta; and finally, the K wave corresponds to the second negative deflection associated to the descending slope of femoral pulse, synchronized with the second heart's sound, and so with semilunar valves' closure. The RK interval represents the systolic phase, while the complementary KR interval represents the diastolic period.

The following temporal parameters were extracted and normalized by the corresponding RR duration, in order to describe the relative time occurrence of the main BCG events: RI, RJ, RK and IK sub-intervals. In addition, the peak-to-peak amplitude parameters A_{HI}, A_{IJ} and A_{JK} were

computed. They are inertial forces in nature, so that it was deemed reasonable to normalize them by the subject's body mass index (BMI).

2.5. Statistical analysis

Due to non-Gaussian distribution of the temporal and amplitude parameters, data were presented as median and 25th and 75th percentiles, unless otherwise specified. To evaluate changes in BCG signals induced by the imposed breathing manoeuvres, non-parametric paired Wilcoxon rank test was applied to both temporal (RR, RI, RJ, RK and IK) and amplitude parameters (A_{HI}, A_{IJ} and A_{JK}) to compare the resting condition and each one of the breathing manoeuvres: full-lung apnea, empty-lung apnea, and Valsalva. To test the effects of posture, non-parametric paired Wilcoxon rank test was also applied between the corresponding SUP and ST values for each parameter. Additionally, the same test was applied to test the null hypothesis that empty- and full-lungs apneas generated a similar response on the examined parameters. Null hypothesis was rejected when $p \leq 0.05$.

3. Results

An example of the WA computed in one subject and during each of the studied manoeuvres and postures is shown in Figure 4. In each panel, the red waveform, corresponding to each different tested condition is superimposed to the waveform corresponding to the spontaneous breathing (Rest) condition, represented as blue dashed line. In this case, it is possible to observe how the RR duration was reduced in ST posture compared to SUP posture. In all cases it was also longer in Rest than in the other breathing manoeuvres, as expected from physiology.

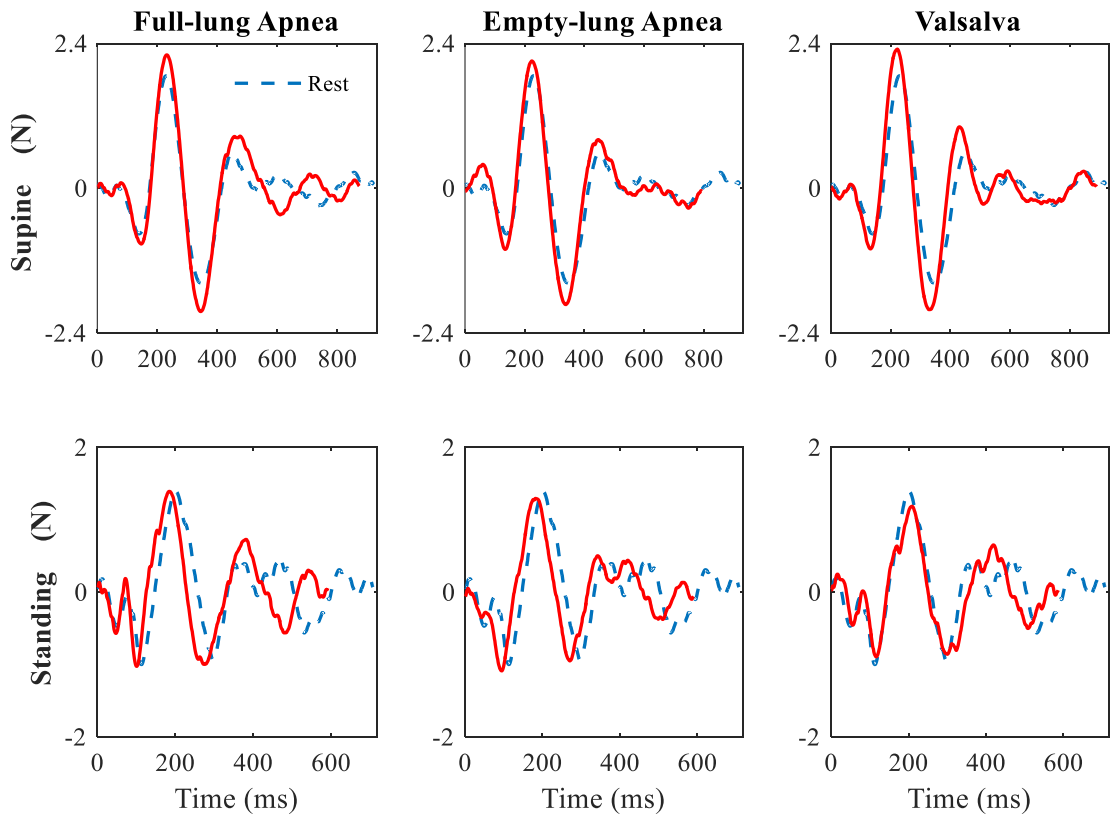

Figure 5: An example of warped average waveforms computed from one subject at each respiratory condition in both SUP (upper panels) and ST (bottom panels) positions. Blue dashed line corresponds to the WA at Rest condition.

The results of the studied normal population in terms of normalized BCG sub-intervals and peak-to-peak amplitudes are shown in Figure 5 and 6, respectively, while their absolute values are reported in table 2.

Table 2. Sub-intervals and peak-to-peak amplitudes in absolute values, expressed as median (25^{th},75^{th} percentile), for each posture (supine and standing, SUP and ST respectively) and during each manoeuvre (rest, full-lung and empty-lung apneas and Valsalva).

	Rest		**Full**		**Empty**		**Val**	
	SUP	**ST**	**SUP**	**ST**	**SUP**	**ST**	**SUP**	**ST**
RR (ms)	922 (777,1007)	675$^{\#}$ (603,755)	847* (695,984)	593*$^{\#}$ (467,694)	789* (669,862)	591*$^{\#}$ (503,667)	752* (691,886)	578*$^{\#}$ (504,644)
RI (ms)	147 (132,161)	123$^{\#}$ (105,143)	146 (131,176)	101*$^{\#}$ (84,125)	154 (132,176)	106*$^{\#}$ (99,115)	151 (131,179)	125*$^{\#}$ (110,157)
RJ (ms)	233 (219,260)	204$^{\#}$ (180,237)	231 (205,272)	188*$^{\#}$ (173,214)	237 (215,277)	183*$^{\#}$ (172,217)	242 (220,268)	203$^{\#}$ (182,226)
RK (ms)	344 (314,370)	298$^{\#}$ (270,324)	344* (311,388)	277*$^{\#}$ (253,313)	340 (320,401)	272*$^{\#}$ (253,305)	346 (324,378)	288$^{\#}$ (268,330)
IK (ms)	197 (184,215)	171$^{\#}$ (162,178)	196* (177,209)	173$^{\#}$ (154,194)	196* (185,212)	166$^{\#}$ (153,182)	191 (180,220)	163$^{\#}$ (148,177)
A_{HI} (N)	1.11 (0.93,1.45)	1.41$^{\#}$ (1.18,1.72)	1.10 (0.82,1.62)	1.40 (1.26,1.79)	1.41* (1.16,1.96)	1.46 (1.14,1.66)	1.26 (0.91,1.85)	1.71$^{\#}$ (1.24,2.22)
A_{IJ} (N)	2.56 (2.20,3.13)	2.74 (2.34,3.41)	2.85 (2.40,3.38)	3.02 (2.48,3.76)	3.19* (2.84,4.05)	3.25 (2.44,3.79)	2.84 (2.29,3.30)	3.14* (2.36,3.89)
A_{JK} (N)	3.08 (2.70,3.96)	2.49$^{\#}$ (2.14,2.88)	3.32 (2.68,4.20)	3.02* (2.46,4.29)	3.83* (2.96,4.31)	3.14$^{\#}$* (2.61,3.69)	3.60 (3.17,3.83)	3.02* (2.36,4.30)

*: $p \leq 0.05$ vs Rest;
#: $p \leq 0.05$ SUP vs ST.

As previously observed, the RR interval was shortened for each respiratory manoeuvre with respect to the Rest condition, with significantly shorter values in ST posture compared to SUP, as expected (see Figure 5, upper panel).

Regarding BCG-derived normalized subintervals, in SUP posture the respiratory manoeuvres affected the I, J and K time occurrence by prolonging the corresponding temporal parameters in empty-lung apnea (RI +19%, RK +15%, RJ +16%, IK +11%) and Valsalva (RI +26%, RK +13%, RJ +21%, IK +11%), expressed as % variation compared to the Rest value, while full-lung apnea affected only RI (+7%).

In ST posture, empty-lung apnea did not significantly modify any parameter, while full-lung apnea prolonged all sub-intervals (RK +9%, RJ +9%, IK +10%) except RI. In the same posture the Valsalva manoeuvre prolonged all sub-intervals (RI +24%, RK +17%, RJ +11%) except IK. When comparing SUP vs ST conditions, the majority of parameters resulted shortened in SUP. This was particularly evident for the IK interval, which was always shorter in SUP than in ST.

Finally, when comparing the two apneas (Full and Emp), all temporal parameters (RR, RI, RJ, RK, IK) were significantly different between these two conditions ($p<0.05$ in all cases) in supine position, whereas no significant differences were found while standing.

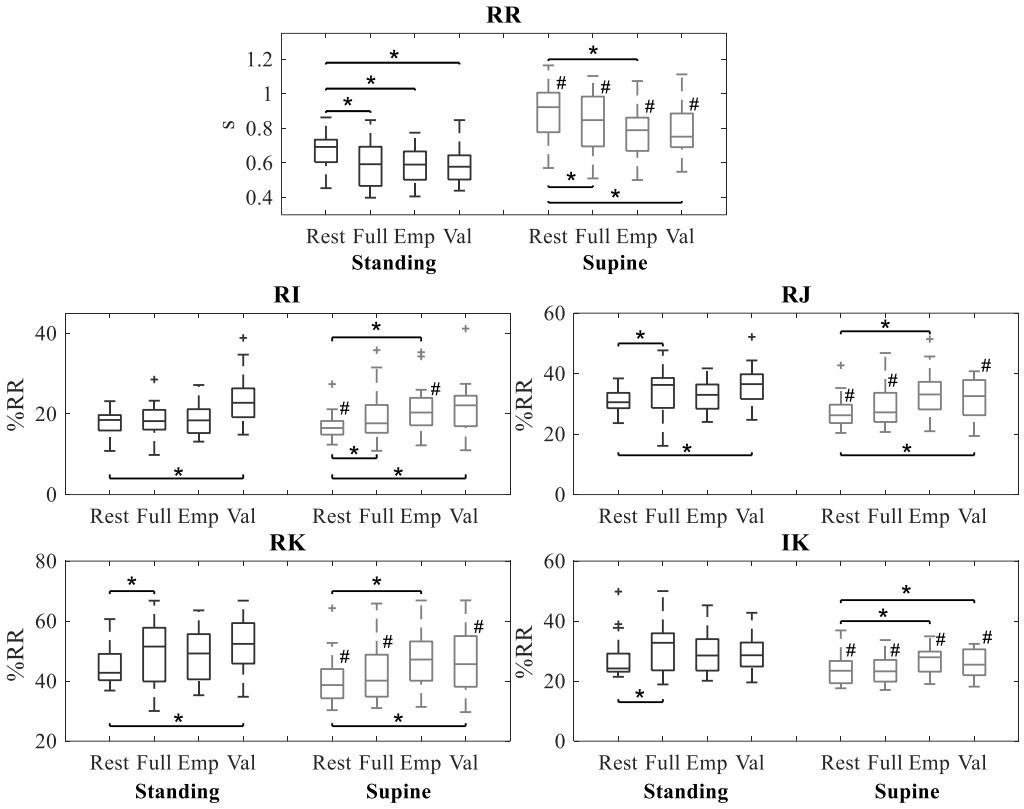

Figure 6: Results of RR and normalized sub-intervals obtained in the normal population of 20 subjects represented as Whisker plots. *:p≤0.05 vs Rest; #:p≤0.05 SUP vs ST.

As regards normalized peak-to-peak amplitudes, in SUP the only respiratory manoeuvre that affected all the indices compared to Rest was the empty-lung apnea (A_{HI} +25%, A_{IJ} +17%, A_{JK} +17%).

In ST posture, A_{HI} resulted unchanged, A_{IJ} increased by 13% only with Valsalva, while A_{JK} resulted incremented by 20% as a result of each manoeuvre. Compared to ST, the main differences in SUP were found in Rest with a decrease in A_{HI} and an increase in A_{JK} peak-to-peak amplitudes. In addition, A_{HI} was found to be decreased also during Valsalva manoeuvre.

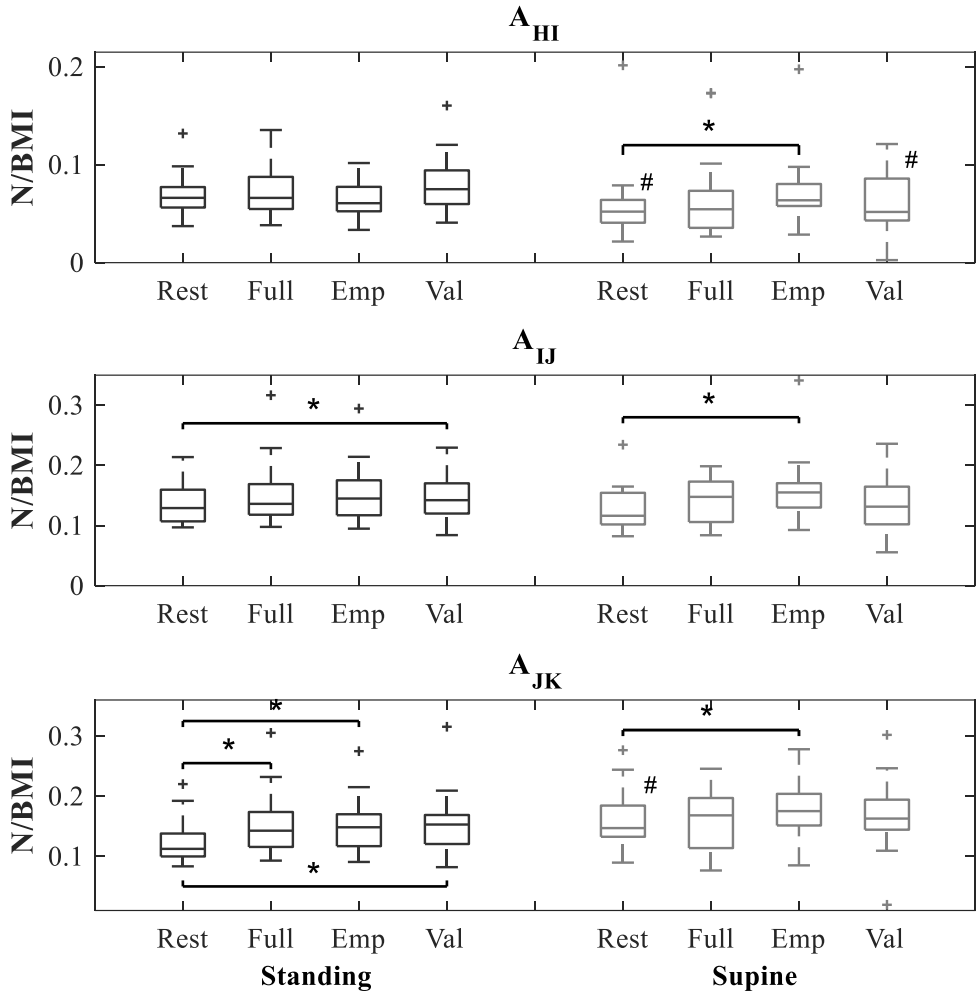

Figure 7: Results of normalized peak-to-peak amplitudes obtained in the normal population of 20 subjects represented as Whisker plots. *:p≤0.05 vs Rest; #:p≤0.05 vs Standing.

4. Discussion and conclusion

Ballistocardiography has been originally proposed as a diagnostic tool to study cardiac mechanics and obtain information about cardiac contractility by measuring the shifting in the body mass centre due to displacements of the heart, as well as of the blood masses in the vessels due to cardiac contractions (Gubner et al., 1953; Starr, 1965, 1955; Starr et al., 1939). However, the limited technology available during its early developments and the large inter-subject variability of the signal impeded to achieve a generalized usage.

More recently, new developments in accelerometer technology and hardware miniaturization led to the reconsideration of BCG as a potentially useful non-invasive methodology to characterize cardiac performance (Inan et al., 2015). In fact, this technique potentially offers a simple, efficient and affordable solution for home e-health monitoring as it can be embedded in commonly-used objects (i.e., weighting scale, bed, sitting chair). In particular, the RJ interval has been proposed as surrogate of the pre-ejection period (PEP) (Etemadi et al., 2011; Inan et

al., 2009; Javaid et al., 2016), a non-invasive indirect measurement of cardiac contractility (Lewis et al., 1977) and, combined with photoplethysmography (PPG), both I and J time occurrences have been shown to be an accurate estimate of arterial stiffening (Wiard, 2012).

In this perspective, it becomes important to define a range of values from a normal population for both temporal and amplitude parameters that can be extracted from the BCG, and to study their changes related to posture or respiratory manoeuvres. This information could reveal its utility both in the definition of a specific acquisition protocol, and in revealing pathologic or physiologically-induced alterations.

In our work, we aimed at studying the BCG signal obtained by a force platform in a population of normal subjects in different cardiac preload and afterload conditions, as well as different autonomic control activity, by means of changes in posture (supine and standing) and by different simple respiratory protocols (normal breathing, apnea and Valsalva).

Indeed, respiration is one of the strongest modulator of cardiac function, as a consequence of changes in intra-thoracic pressure and systemic venous return (Guyton and Hall, 2006). In particular, with the Valsalva manoeuvre a sequence of rapid changes in preload and afterload stress is induced. More precisely, it has a direct influence on the pattern of the cardiovascular system, whose response has been reported to be subdivided into four phases (Hamilton et al., 1936; Looga, 2005): in the early phases of strain (I-II), the increase in intrathoracic pressure results in a concomitant increase in both heart rate and blood pressure (Porth et al., 1984); this is followed by a an increase in parasympathetic activity after strain release (phases III and IV), resulting in a decrease in heart rate.

Apneas performed at end-inspiration and at end-expiration are related to different intrathoracic pressures and non-modulated venous return, giving the possibility to acquire the BCG signal in a relatively steady-state condition. However, the cardiovascular response during these manoeuvres has been reported to be variable over time: Javorka and colleagues showed how an empty-lung apnea induced an initial tachycardia in the first 10 seconds approximately, followed by a compensatory decrease in heart rate, evaluated in 24 young healthy volunteers while in sitting position (Javorka et al., 2001). Results of our work revealed that the empty-lungs apnea resulted in a different outcome in temporal parameters, compared to full-lung apnea, but only in supine position. This could be due to the fact that in standing, the initial control condition before the apnea was already manifesting a sympathetic activation (median RRrest= 675 ms in standing, vs. 922 ms in supine), thus limiting the additional effects of the provoking manoeuvre.

Our results confirmed that acquisition of BCG from a piezoelectric load cells force platform was feasible in all subjects, and signal quality allowed for further analysis and automated parameters extraction in both examined postural conditions.

The acquired BCG is a quasi-periodic signal characterized by a large inter-beat variability in morphology (both in duration and amplitude). Based on these signal characteristics, DTW was selected as the most appropriate averaging method and it was applied to 32-beat sequences obtained during the different breathing manoeuvres imposed. This number of consecutive beats was determined as a compromise between the requirement of acquiring an adequate number of waveforms to be included in the warped averaging in order to improve the signal-to-noise ratio, and the need to keep as short as possible the acquisition in an hypothetical user-driven scenario in which the subject has to maintain the suggested posture for a limited time, both during spontaneous breathing and respiratory manoeuvres. In particular, during Valsalva manoeuvre,

this choice resulted in focusing our analysis to the effects relevant to the early phases of the cardiovascular response. Also for apneas, the choice to limit our analysis to the first 32 beats acquired during this manoeuvre led to a predominance of the initial tachycardia in the observed results. To our knowledge, this is the first time that DTW technique is applied to the BCG signal with the goal of generating normality ranges in different postural and breathing manoeuvres.

The DTW method resulted in an averaged waveform in both duration and amplitude from which both temporal and peak-to-peak amplitude parameters were automatically extracted. In order to obtain a range of comparable results representative of the studied normal population, two different normalizations were introduced: for temporal indices, each sub-interval parameter was normalized by the corresponding heart beat duration; for amplitude indices, each peak-to-peak parameter was normalized by the subject BMI. Normalization by the heart beat duration allowed pooling subjects for comparison of temporal BCG parameters between SUP and ST postures, despite heart rate was found increased while in standing posture, as well as between the resting spontaneous respiration and each breathing manoeuvre. Similarly, normalization by the BMI intrinsically corrected for possible inter-subject variability due to different stroke volume and cardiac output, thus allowing cumulative analysis without other distinctions (i.e. sex, body composition) (Collis et al., 2001).

Obtained results showed modifications in both amplitude and duration BCG-derived parameters among the respiratory manoeuvres, especially when compared to spontaneous breathing, but being also dependent on the assumed posture. The prolongation of RJ interval during Valsalva, which could be explained as a consequence of the decreased venous return during the strain, was already reported in the literature (Inan et al., 2008). However, this decrease in venous return was not visible in terms of amplitudes, in contrast to the reduced values of A_{IJ} reported in (Inan et al., 2009).

On the other hand, the observed reduction in the RJ interval from standing to supine is likely due to the increase in venous return associated to the supine condition, which is also manifested by a decrease in the pre-ejection period. This is in agreement with what was observed by McCall et al. by studying subjects in standing position on a weighting scale by comparing results on ground and during microgravity induced by parabolic flight manoeuvre (McCall et al., 2014). The increase in venous return as a characteristic of the supine condition, associated also to a larger stroke volume (Frey et al., 1994), might also be reflected in the larger peak-to-peak A_{JK} amplitude as observed in supine compared to standing.

These observations demonstrate the complex interaction between intrathoracic pressure changes acting on venous return, the effect of hydrostatic pressure gradient elicited by postural conditions, and the autonomic nervous system modulation on the heart rate and peripheral baroreceptor reflex.

As these contributions cannot be easily disentangled, the availability of normality reference values for each condition to be used as comparison of new subjects assumes particular importance in the potential identification of possible pathologies involving mechano-electrical cardio-pulmonary coupling.

In conclusion, an acquisition protocol for the BCG signal that included different respiratory manoeuvres to be performed in standing or supine position was implemented. The acquired signal was analyzed by DTW to compute normality ranges in both temporal and amplitude parameters, and to evaluate potential changes induced by the different settings. Results show

dependency from respiratory manoeuvre and posture, supporting the need for definition of separate normality ranges for each of the studied conditions, as well as the importance of applying specific manoeuvres to highlight any pathological response in the computed BCG parameters.

Acknowledgments

This research was supported by the Italian Space Agency (contract 2013-064-R.0, PI Enrico Caiani). This work was supported also by project DPI2016-75458-R funded by MINECO (Spain) and FEDER, and by Gobierno de Aragón and European Social Fund (EU) through BSICoS Group (T96). The CIBER in Bioengineering, Biomaterials & Nanomedicine (CIBER-BBN) is an initiative of Instituto de Salud Carlos III (Spain). P-F Migeotte is supported by the Belgian Federal Science Policy Office (BELSPO) via the ESA PRODEX program.

References

Aunon, J., McGillem, C., Childers, D., 1980. Signal processing in evoked potential research: averaging and modeling. Crit. Rev. Bioeng. 5, 323–367.

Caiani, E.G., Porta, A., Baselli, G., Turiel, M., Muzzupappa, S., Pagani, M., Malliani, A., Cerutti, S., 2002. Analysis of cardiac left-ventricular volume based on time warping averaging. Med. Biol. Eng. Comput. 40, 225–233.

Cohen, A., 1986. Biomedical signal processing. Boca Raton, Fla. CRC Press.

Collis, T., Devereux, R.B., Roman, M.J., Simone, G. de, Yeh, J.-L., Howard, B.V., Fabsitz, R.R., Welty, T.K., 2001. Relations of Stroke Volume and Cardiac Output to Body Composition. Circulation 103, 820–825. doi:10.1161/01.CIR.103.6.820

Etemadi, M., Inan, O.T., Giovangrandi, L., Kovacs, G.T.A., 2011. Rapid Assessment of Cardiac Contractility on a Home Bathroom Scale. IEEE Trans. Inf. Technol. Biomed. 15, 864–869. doi:10.1109/TITB.2011.2161998

Frey, M.A.B., Tomaselli, C.M., Hoffler, W.G., 1994. Cardiovascular Responses to Postural Changes: Differences with Age for Women and Men. J. Clin. Pharmacol. 34, 394–402. doi:10.1002/j.1552-4604.1994.tb04979.x

Gubner, R.S., Rodstein, M., Ungerleider, H.E., 1953. Ballistocardiography; an appraisal of technic, physiologic principles, and clinical value. Circulation 7, 268–286.

Guyton, A.C., Hall, J.E., 2006. Textbook of Medical Physiology, 11th edition. ed. Elsevier Saunders, Philadelphia.

Hamilton, W.F., Woodbury, R.A., Harper, H.T., 1936. PHYSIOLOGIC RELATIONSHIPS BETWEEN INTRATHORACIC, INTRASPINAL AND ARTERIAL PRESSURES. J. Am. Med. Assoc. 107, 853–856. doi:10.1001/jama.1936.02770370017005

He, D.D., Winokur, E.S., Sodini, C.G., 2011. A continuous, wearable, and wireless heart monitor using head ballistocardiogram (BCG) and head electrocardiogram (ECG), in: 2011 Annual International Conference of the IEEE Engineering in Medicine and Biology Society, EMBC. Presented at the 2011 Annual International Conference of the IEEE Engineering in Medicine and Biology Society, EMBC, pp. 4729–4732. doi:10.1109/IEMBS.2011.6091171

Inan, O.T., Etemadi, M., Wiard, R.M., Giovangrandi, L., Kovacs, G.T.A., 2009. Robust ballistocardiogram acquisition for home monitoring. Physiol. Meas. 30, 169. doi:10.1088/0967-3334/30/2/005

Inan, O.T., Etemadi, M., Wiard, R.M., Kovacs, G.T.A., Giovangrandi, L., 2008. Non-invasive measurement of Valsalva-induced hemodynamic changes on a bathroom scale Ballistocardiograph, in: 2008 30th Annual International Conference of the IEEE Engineering in Medicine and Biology Society. Presented at the 2008 30th Annual International Conference of the IEEE Engineering in Medicine and Biology Society, pp. 674–677. doi:10.1109/IEMBS.2008.4649242

Inan, O.T., Migeotte, P.-F., Park, K.-S., Etemadi, M., Tavakolian, K., Casanella, R., Zanetti, J., Tank, J., Funtova, I., Prisk, G.K., Di Rienzo, M., 2015. Ballistocardiography and seismocardiography: a review of recent advances. IEEE J. Biomed. Health Inform. 19, 1414–1427. doi:10.1109/JBHI.2014.2361732

Javaid, A.Q., Ashouri, H., Tridandapani, S., Inan, O.T., 2016. Elucidating the Hemodynamic Origin of Ballistocardiographic Forces: Toward Improved Monitoring of Cardiovascular Health at Home. IEEE J. Transl. Eng. Health Med. 4, 1–8. doi:10.1109/JTEHM.2016.2544752

Javorka, M., Žila, I., Javorka, K., Čalkovská, A., 2001. "Respiratory" oscillations of cardiovascular parameters during voluntary apnea. Respir. Physiol. 126, 251–254. doi:10.1016/S0034-5687(01)00229-8

Lewis, R.P., Rittogers, S.E., Froester, W.F., Boudoulas, H., 1977. A critical review of the systolic time intervals. Circulation 56, 146–158. doi:10.1161/01.CIR.56.2.146

Looga, R., 2005. The Valsalva manoeuvre—cardiovascular effects and performance technique: a critical review. Respir. Physiol. Neurobiol. 147, 39–49. doi:10.1016/j.resp.2005.01.003

Martinez, J.P., Almeida, R., Olmos, S., Rocha, A.P., Laguna, P., 2004. A wavelet-based ECG delineator: evaluation on standard databases. IEEE Trans. Biomed. Eng. 51, 570–581. doi:10.1109/TBME.2003.821031

McCall, C., Stuart, Z., Wiard, R.M., Inan, O.T., Giovangrandi, L., Cuttino, C.M., Kovacs, G.T.A., 2014. Standing ballistocardiography measurements in microgravity, in: 2014 36th Annual International Conference of the IEEE Engineering in Medicine and Biology Society. Presented at the 2014 36th Annual International Conference of the IEEE Engineering in Medicine and Biology Society, pp. 5180–5183. doi:10.1109/EMBC.2014.6944792

Pinheiro, E., Postolache, O., Girão, P., 2010. Theory and Developments in an Unobtrusive Cardiovascular System Representation: Ballistocardiography. Open Biomed. Eng. J. 4, 201–216. doi:10.2174/1874120701004010201

Porth, C.J., Bamrah, V.S., Tristani, F.E., Smith, J.J., 1984. The Valsalva maneuver: mechanisms and clinical implications. Heart Lung J. Crit. Care 13, 507–518.

Sakoe, H., Chiba, S., 1978. Dynamic programming algorithm optimization for spoken word recognition. IEEE Trans. Acoust. Speech Signal Process. 26, 43–49. doi:10.1109/TASSP.1978.1163055

Shin, J.H., Hwang, S.H., Chang, M.H., Park, K.S., 2011. Heart rate variability analysis using a ballistocardiogram during Valsalva manoeuvre and post exercise. Physiol. Meas. 32, 1239. doi:10.1088/0967-3334/32/8/015

Starr, I., 1965. Progress Towards a Physiological Cardiology. A Second Essay on the Ballistocardiogram. Ann. Intern. Med. 63, 1079–1105. doi:10.7326/0003-4819-63-6-1079

Starr, I., 1955. Normal Standards for Amplitude of Ballistocardiograms Calibrated by Force. Circulation 11, 914–926. doi:10.1161/01.CIR.11.6.914

Starr, I., Rawson, A.J., Schroeder, H.A., Joseph, N.R., 1939. Studies on the estimation of cardiac output in man, and of abnormalities in cardiac function. Am. Heart J. 18, 506. doi:10.1016/S0002-8703(39)90682-4

Wiard, R.M., 2012. Validation of non-invasive standing arterial stiffness measurements using ballistocardriography and photoplethysmography.

Zhu, X., Chen, W., Kitamura, K., Nemoto, T., 2012. Comparison of pulse rate variability indices estimated from pressure signal and photoplethysmogram, in: 2012 IEEE-EMBS International Conference on Biomedical and Health Informatics (BHI). Presented at the 2012 IEEE-EMBS International Conference on Biomedical and Health Informatics (BHI), pp. 867–870. doi:10.1109/BHI.2012.6211725

TABLES

Table 1: Study population characteristics expressed as mean ± std.

Variable	Males	Females
Age (years)	32.9 ± 9.0	28.2 ± 4.8
Weight (kg)	72.9 ± 10.5	53.9 ± 8.3
Height (m)	1.79 ± 0.08	1.62 ± 0.06
BMI (kg/m^2)	22.8 ± 4.06	20.6 ± 2.13

BMI: body mass index.

Table 2. Sub-intervals and peak-to-peak amplitudes in absolute values, expressed as median (25^{th},75^{th} percentile), for each posture (supine and standing, SUP and ST respectively) and during each manoeuvre (rest, full-lung and empty-lung apneas and Valsalva).

	Rest		Full		Empty		Val	
	SUP	**ST**	**SUP**	**ST**	**SUP**	**ST**	**SUP**	**ST**
RR (ms)	922 (777,1007)	675# (603,755)	847* (695,984)	593*# (467,694)	789* (669,862)	591*# (503,667)	752* (691,886)	578*# (504,644)
RI (ms)	147 (132,161)	123# (105,143)	146 (131,176)	101*# (84,125)	154 (132,176)	106*# (99,115)	151 (131,179)	125*# (110,157)
RJ (ms)	233 (219,260)	204# (180,237)	231 (205,272)	188*# (173,214)	237 (215,277)	183*# (172,217)	242 (220,268)	203# (182,226)
RK (ms)	344 (314,370)	298# (270,324)	344* (311,388)	277*# (253,313)	340 (320,401)	272*# (253,305)	346 (324,378)	288# (268,330)
IK (ms)	197 (184,215)	171# (162,178)	196* (177,209)	173# (154,194)	196* (185,212)	166# (153,182)	191 (180,220)	163# (148,177)
$\mathbf{A_{HI}}$ (N)	1.11 (0.93,1.45)	1.41# (1.18,1.72)	1.10 (0.82,1.62)	1.40 (1.26,1.79)	1.41* (1.16,1.96)	1.46 (1.14,1.66)	1.26 (0.91,1.85)	1.71# (1.24,2.22)
$\mathbf{A_{IJ}}$ (N)	2.56 (2.20,3.13)	2.74 (2.34,3.41)	2.85 (2.40,3.38)	3.02 (2.48,3.76)	3.19* (2.84,4.05)	3.25 (2.44,3.79)	2.84 (2.29,3.30)	3.14* (2.36,3.89)
$\mathbf{A_{JK}}$ (N)	3.08 (2.70,3.96)	2.49# (2.14,2.88)	3.32 (2.68,4.20)	3.02* (2.46,4.29)	3.83* (2.96,4.31)	3.14#* (2.61,3.69)	3.60 (3.17,3.83)	3.02* (2.36,4.30)

*: $p \leq 0.05$ vs Rest;

#: $p \leq 0.05$ SUP vs ST.

FIGURE LEGENDS

Figure 1: Schematic of the experimental set up for the subject in standing position (a) and in supine (b).

Figure 2: Example of synchronized ECG (mV) and the three components of the BCG signal: HF (head-to-foot), AP (antero-posterior) and LR (left-to-right) components (N), in both supine (left) and standing (right) positions..

Figure 3: Example of the computed time-warping function (TWF) that best aligns the two consecutive BCG normalized waveforms, here denoted as $S_x(i)$ and $S_y(j)$.

Figure 4: Example of a sequence of 32 BCG waveforms (light blue) obtained in one subject, the result of their synchronous averaging (dark blue dashed line) and of the DTW averaging (in red).

Figure 5: An example of warped average waveforms computed from one subject at each respiratory condition in both SUP (upper panels) and ST (bottom panels) positions. Blue dashed line corresponds to the WA at Rest condition.

Figure 6: Results of RR and normalized sub-intervals obtained in the normal population of 20 subjects represented as Whisker plots. *:p≤0.05 vs Rest; #:p≤0.05 SUP vs ST.

Figure 7: Results of normalized peak-to-peak amplitudes obtained in the normal population of 20 subjects represented as Whisker plots. *:p≤0.05 vs Rest; #:p≤0.05 vs Standing.

FIGURES

Figure 1.

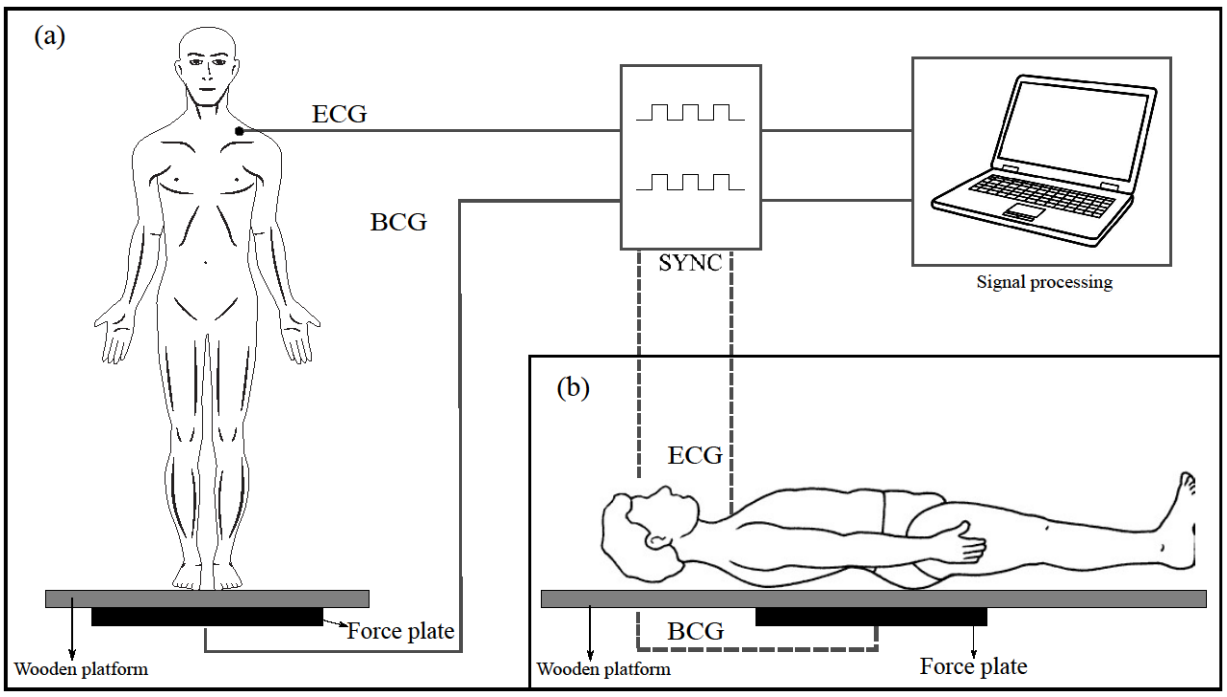

Figure 2.

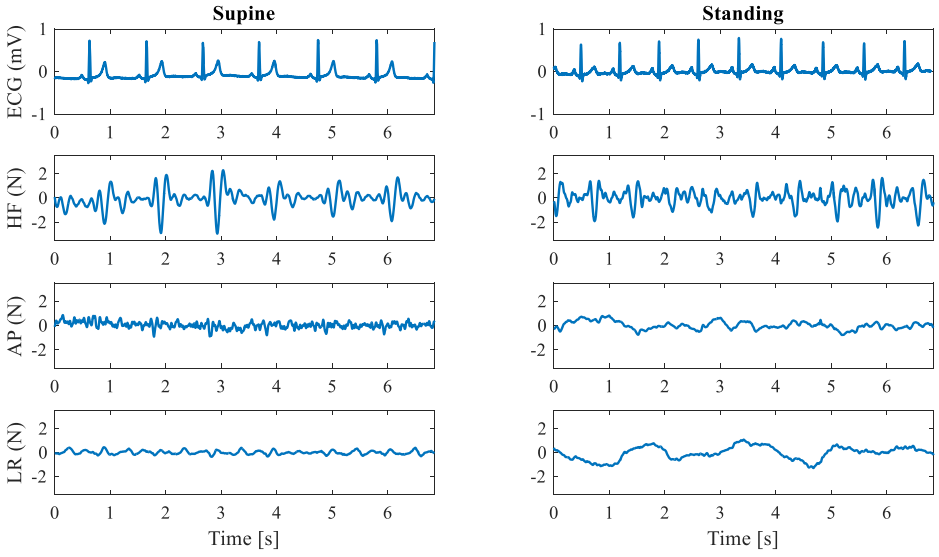

Figure 3.

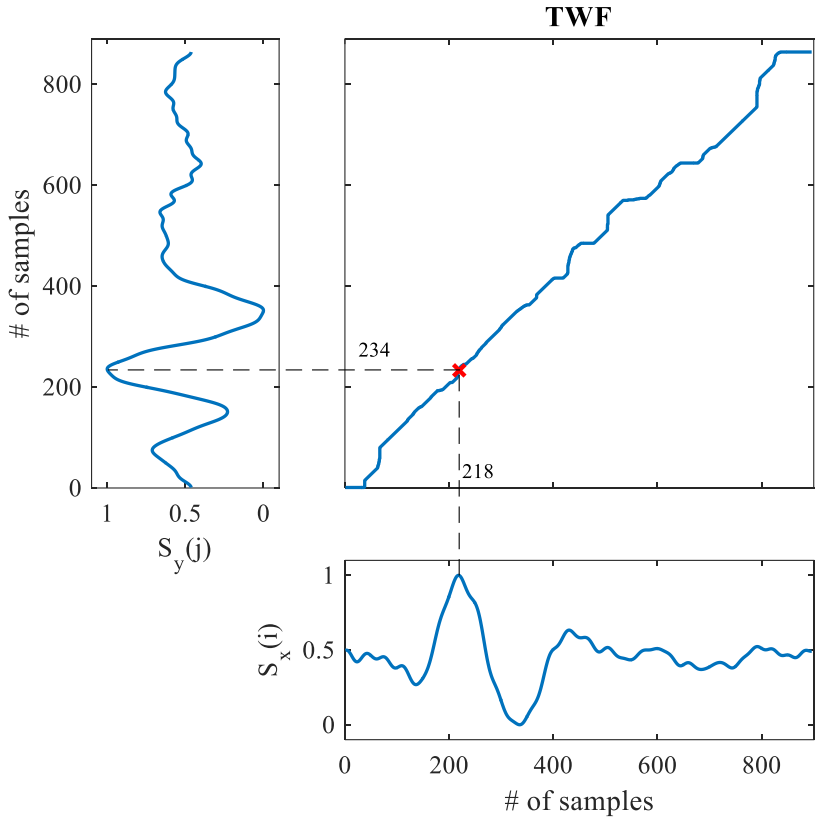

Figure 4.

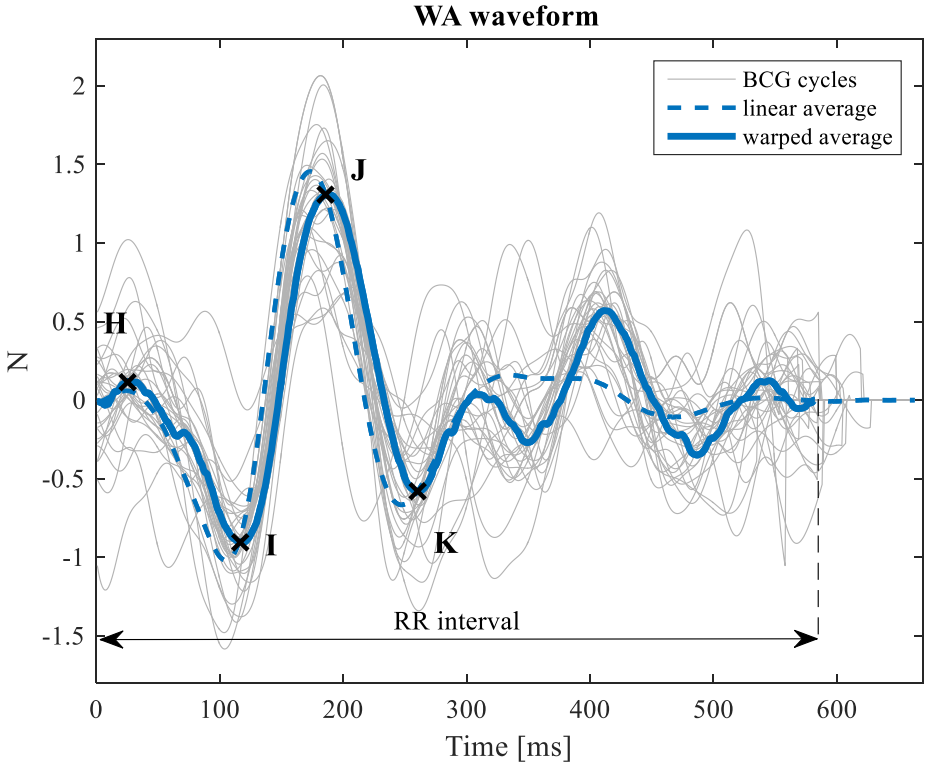

Figure 5.

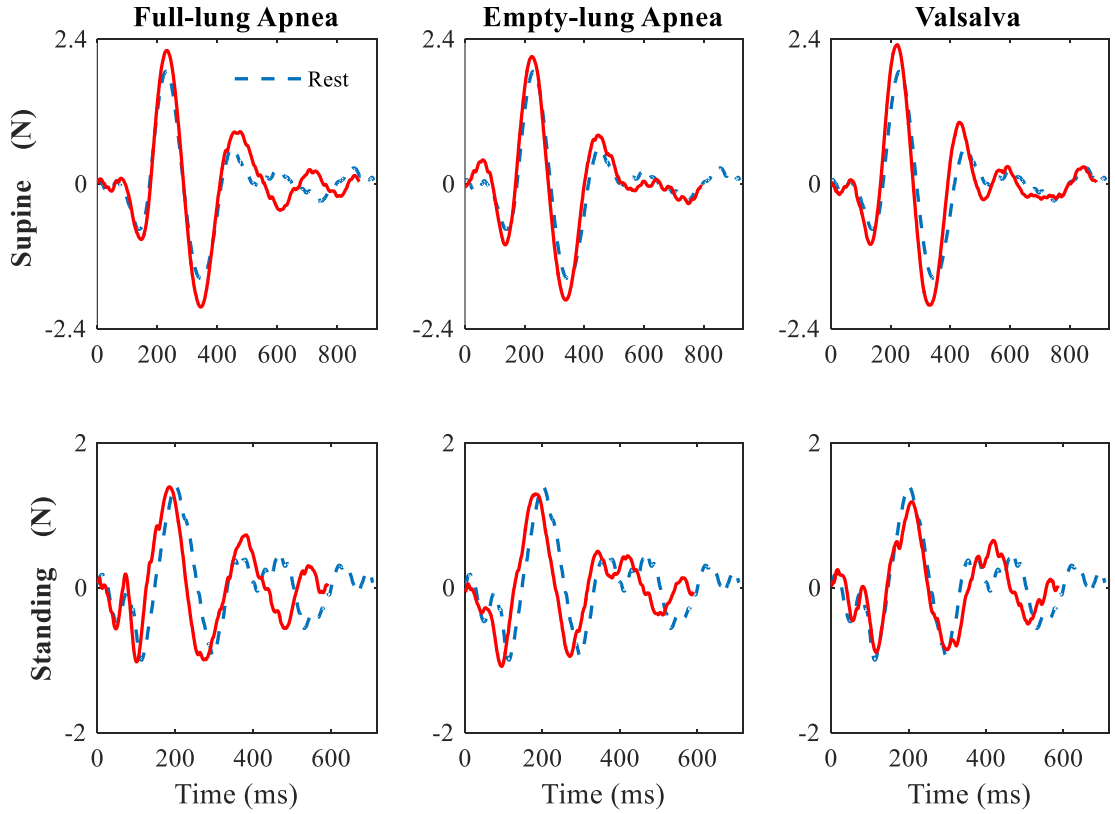

Figure 6.

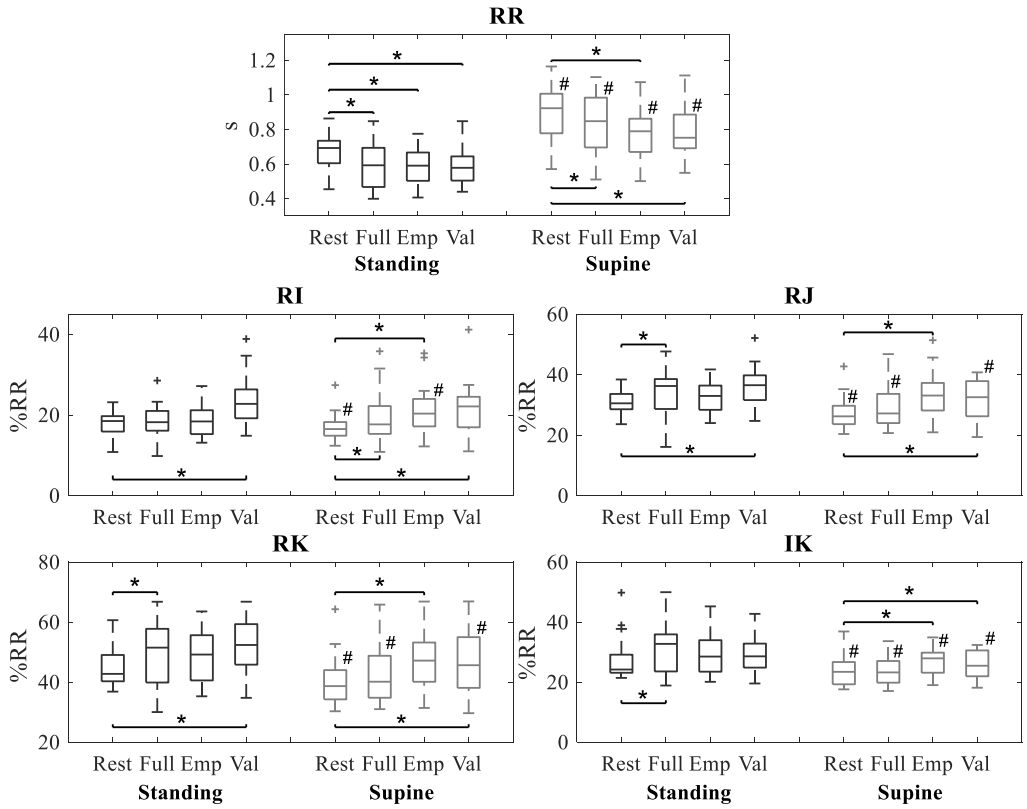

Figure 7.